



Biofilm Interaction Mapping and Analysis (BIMA) of Interspecific Interactions in *Pseudomonas* Co-culture Biofilms

Suzanne M. Kosina¹, Peter Rademacher^{1†}, Kelly M. Wetmore¹, Markus de Raad¹, Marcin Zemla^{1†}, Grant M. Zane², Jennifer J. Zulovich², Romy Chakraborty¹, Benjamin P. Bowen^{1,3}, Judy D. Wall², Manfred Auer¹, Adam P. Arkin¹, Adam M. Deutschbauer¹ and Trent R. Northen^{1,3*}

OPEN ACCESS

Edited by:

Maria I. Klapa,
Institute of Chemical Engineering
Sciences, Greece

Reviewed by:

Chien-Yi Chang,
Newcastle University, United Kingdom
Devendra Dusane,
Nationwide Children's Hospital,
United States

*Correspondence:

Trent R. Northen
trnorthen@lbl.gov

† Present address:

Peter Rademacher,
DiCe Molecules, South
San Francisco, CA, United States
Marcin Zemla,
Molecular Devices, San Jose, CA,
United States

Specialty section:

This article was submitted to
Systems Microbiology,
a section of the journal
Frontiers in Microbiology

Received: 12 August 2021

Accepted: 04 November 2021

Published: 09 December 2021

Citation:

Kosina SM, Rademacher P,
Wetmore KM, de Raad M, Zemla M,
Zane GM, Zulovich JJ,
Chakraborty R, Bowen BP, Wall JD,
Auer M, Arkin AP, Deutschbauer AM
and Northen TR (2021) Biofilm
Interaction Mapping and Analysis
(BIMA) of Interspecific Interactions in
Pseudomonas Co-culture Biofilms.
Front. Microbiol. 12:757856.
doi: 10.3389/fmicb.2021.757856

¹ Environmental Genomics and Systems Biology, Lawrence Berkeley National Laboratory, Berkeley, CA, United States, ² Department of Biochemistry, University of Missouri, Columbia, MO, United States, ³ Lawrence Berkeley National Laboratory, Joint Genome Institute, Berkeley, CA, United States

Pseudomonas species are ubiquitous in nature and include numerous medically, agriculturally and technologically beneficial strains of which the interspecific interactions are of great interest for biotechnologies. Specifically, co-cultures containing *Pseudomonas stutzeri* have been used for bioremediation, biocontrol, aquaculture management and wastewater denitrification. Furthermore, the use of *P. stutzeri* biofilms, in combination with consortia-based approaches, may offer advantages for these processes. Understanding the interspecific interaction within biofilm co-cultures or consortia provides a means for improvement of current technologies. However, the investigation of biofilm-based consortia has been limited. We present an adaptable and scalable method for the analysis of macroscopic interactions (colony morphology, inhibition, and invasion) between colony-forming bacterial strains using an automated printing method followed by analysis of the genes and metabolites involved in the interactions. Using Biofilm Interaction Mapping and Analysis (BIMA), these interactions were investigated between *P. stutzeri* strain RCH2, a denitrifier isolated from chromium (VI) contaminated soil, and 13 other species of *Pseudomonas* isolated from non-contaminated soil. One interaction partner, *Pseudomonas fluorescens* N1B4 was selected for mutant fitness profiling of a DNA-barcoded mutant library; with this approach four genes of importance were identified and the effects on interactions were evaluated with deletion mutants and mass spectrometry based metabolomics.

Keywords: biofilm, mass spectrometry, mutant fitness profiling, consortia, morphology, microbial interaction, metabolomics, exometabolomics

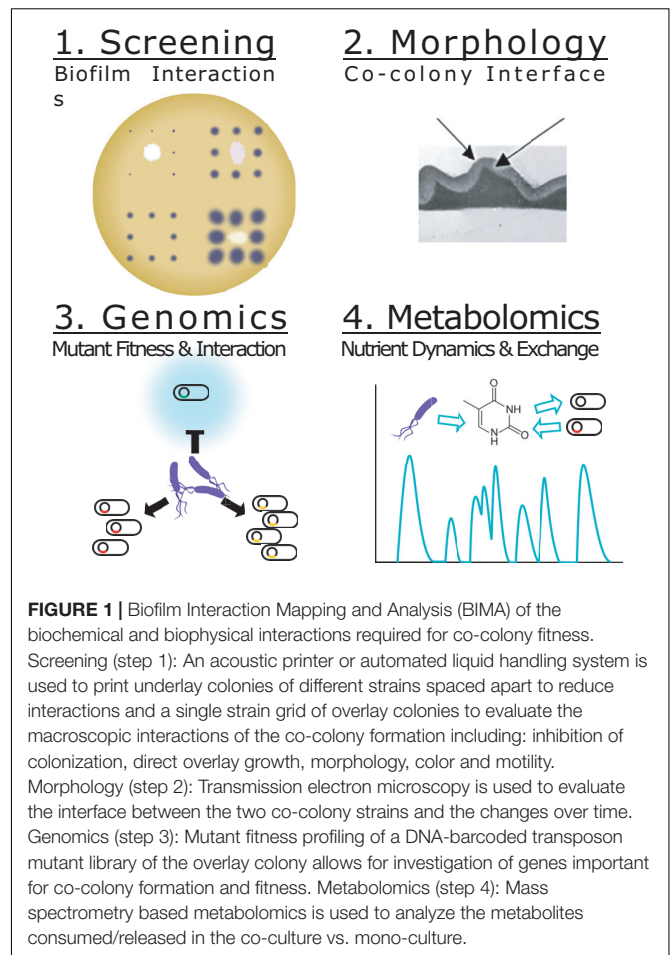
INTRODUCTION

Consortia based systems in biotechnologies are widespread, however, controlling them is challenging due to the genomic and metabolomic complexities of the interactions. Characterization of the genes and metabolites involved in the interactions opens up the possibility for improved consortia functionality by use of engineered strains and culture condition metabolite amendments. Previously, metabolomics of adjacently printed cultures of *P. stutzeri* and *Shewanella oneidensis*

were analyzed using replication-exchange-transfer and nanostructure initiator mass spectrometry; however, this approach does not elucidate the genes important for the interactions (Louie et al., 2013). The ability to incorporate genomics into these types of approaches will allow for a better understanding of the interactions involved. Barcoded mutant libraries are proving to be a powerful tool for the discovery of the genetic determinants of co-culture fitness (Goodman et al., 2011; Kosina et al., 2016). Next-generation sequencing enables rapid profiling of the abundance of barcodes mapped to specific genes in transposon mutant libraries under a wide range of environmental conditions (Wetmore et al., 2015; Price et al., 2018) and when integrated with metabolomics, provides rapid functional assignment of transport and metabolic processes (Baran et al., 2009) important in microbial interactions.

Pseudomonas are a diverse genus of microbes that have been isolated from all over the world of which both beneficial and pathogenic strains have been identified (Peix et al., 2009; Silby et al., 2011). As common soil-dwelling microorganisms, they are important constituents of microbial ecosystems and rhizosphere environments (Garbeva et al., 2004; Sørensen and Nybroe, 2004; Moore et al., 2006; Li et al., 2013). *Pseudomonas stutzeri*, a model denitrifying pseudomonas, can grow in diverse conditions (Lalucat et al., 2006) and its use has been demonstrated in a number of bioremediation processes, including phenol (Jiang et al., 2014), carbon tetrachloride (Sepúlveda-Torres et al., 2002), uranium (Han et al., 2012), polycyclic aromatic hydrocarbons (Moscoso et al., 2012a), and diesel oil (Kaczorek et al., 2012). Additionally, *P. stutzeri* has been identified in and used in a number of consortia-based applications, such as bioremediation (Nguyen et al., 2008; Brodie et al., 2011; Gałazka et al., 2012), wastewater denitrification (Clarens et al., 1998; Liu et al., 2006), aquaculture water quality management (Erna et al., 2013; Deng et al., 2014), as a plant growth promoter for the biocontrol of phytopathogens (Cottyn et al., 2009; Shen et al., 2013), and manufacturing/municipal waste management (Miyahara et al., 2012; Moscoso et al., 2012b). The use of *P. stutzeri* biofilms for various bioremediation efforts has potential benefits in terms of activity and yields for copper removal (Badar et al., 2013), drinking water denitrification (Lazarova et al., 1992) and naphthalene (Zhao et al., 2016), and phenol (Viggiani et al., 2006) degradation. Given this widespread utilization in both microbial consortia systems and biofilms, *P. stutzeri* was selected to demonstrate the deconstruction of its interactions with other pseudomonas in biofilm-based co-cultures into the genetic and chemical aspects influencing the co-colony fitness.

Here we introduce Biofilm Interaction Mapping and Analysis (BIMA), an integrated platform of automated colony printing, barcoded mutant library profiling and metabolomics to discover and deconstruct the interactions within biofilm-based consortia (Figure 1). Overlaid colonies were printed using an automated liquid handling system to investigate the morphological, inhibitory and invasive interactions between *P. stutzeri* and other pseudomonas soil isolates in a lab model for a biofilm-based consortium. The overlaid colonies were further analyzed using transmission electron microscopy to investigate changes in ultrastructural organization at the species interface over



time. Using a DNA-barcoded mutant transposon library of *P. stutzeri* strain RCH2, we identified genes associated with the fitness of the RCH2 in the co-colony. Additionally, exometabolomic analysis was used to evaluate the exchange of metabolites between RCH2 and another pseudomonas strain. We foresee these tools being valuable resources for both the understanding of natural interactions between pseudomonas in microbial communities and in the development of biofilm-based biotechnological applications.

MATERIALS AND METHODS

Bacterial Strains and Growth Conditions

Pseudomonas stutzeri RCH2 was isolated from chromium(VI) contaminated groundwater at the Department of Energy Hanford 100 Area, Benton County, WA (Han et al., 2010). Thirteen additional pseudomonas strains were isolated from Oak Ridge National Laboratory, Field Research Center, TN under conditions indicated in **Supplementary Table 1**. Liquid cultures were inoculated into 3-(N-morpholino)propanesulfonic acid (MOPS) buffered casein yeast magnesium broth (Mb-CYM): 10 g/L pancreatic digest of casein, 5 g/L Difco yeast extract, 1 g/L MgSO₄ heptahydrate, 10 mM MOPS. Mb-CYM agar was prepared with

the addition of 1.5% w/v of agar. Unless otherwise noted, culture conditions were as follows. Strains were maintained as glycerol stocks; revived cultures were plated onto agar plates, incubated at 30°C for 24 h and stored at 4°C. Starter cultures for experiments were prepared from single colonies inoculated into liquid Mb-CYM broth and cultured aerobically with shaking at 30°C overnight. Uninoculated and unstreaked but incubated cultures/plates were used as negative controls for contamination. In figures and text, *Pseudomonas stutzeri* RCH2 is referred to as culture #1, while the 13 other strains are referred to as cultures #2–14, and uninoculated controls as culture #15 as indicated in **Supplementary Table 1**.

Printed Colony Biofilm Morphology Screening Assay

Rectangular petri dishes with ANSI standard dimensions were poured with agar to a height of 5 mm. Overnight cultures of the 14 effector strains (including RCH2) and uninoculated control broth (**Supplementary Table 1**) were diluted 1:50 in fresh Mb-MYM and then added to a 96-well plate. The plates were loaded onto a Hamilton Vantage Liquid Handling System equipped with a 96 pipetting head which was used to dip pipette tips into the liquid cultures and press/print them against the surface of the agar in a grid; a single colony of each unique strain was printed in a 3 × 5 grid (**Figure 2A**). The lidded-plate was sealed with Parafilm and incubated at 30°C for 2 days once visible colonies had formed of similar size (**Supplementary Figure 1**). Printing was repeated using only *P. stutzeri* RCH2 (the interaction strain) in all well positions of a 16 × 24 grid (ANSI standard dimensions of a 384 well plate), excluding the positions from the original print at time 0 (**Figure 2A**). Cultures were incubated for an additional 4 days prior to imaging using a digital camera. Image analysis was performed using ImageJ (Schneider et al., 2012). Briefly, the image was converted to 16-bit grayscale, corrected for uneven lighting using the FFT bandpass filter (filter large structures to 70 pixels and small structures to 5 pixels, 5% tolerance, autoscale and saturate after filtering), auto thresholded to black and white, and then the colonies were measured using the Analyze Particles tool (colonies missed by the automated selection were manually outlined and then measured). Measurements included area and position. Colony areas of surrounding (8 colonies in a square around the center interaction colony) and closest/farthest neighbors (sides/corners of the square) were compared with the colonies surrounding the control uninoculated position (#15) using Dunnett's multiple comparison procedure using R version 3.6.2 (Hothorn et al., 2008; R Core Team, 2014).

Co-colony Overlay Morphology With Light Microscopy and Transmission Electron Microscopy

Overnight culture of *Pseudomonas* sp. FW300-N1B4 (N1B4) was manually pipetted (10 µL) onto an agar plate and incubated at 30°C overnight. Overnight culture of *P. stutzeri* RCH2 was manually pipetted (10 µL) over the top of the N1B4 colony with care to not puncture the colony surface and to avoid allowing the droplet to spill over the sides. For time course analysis of

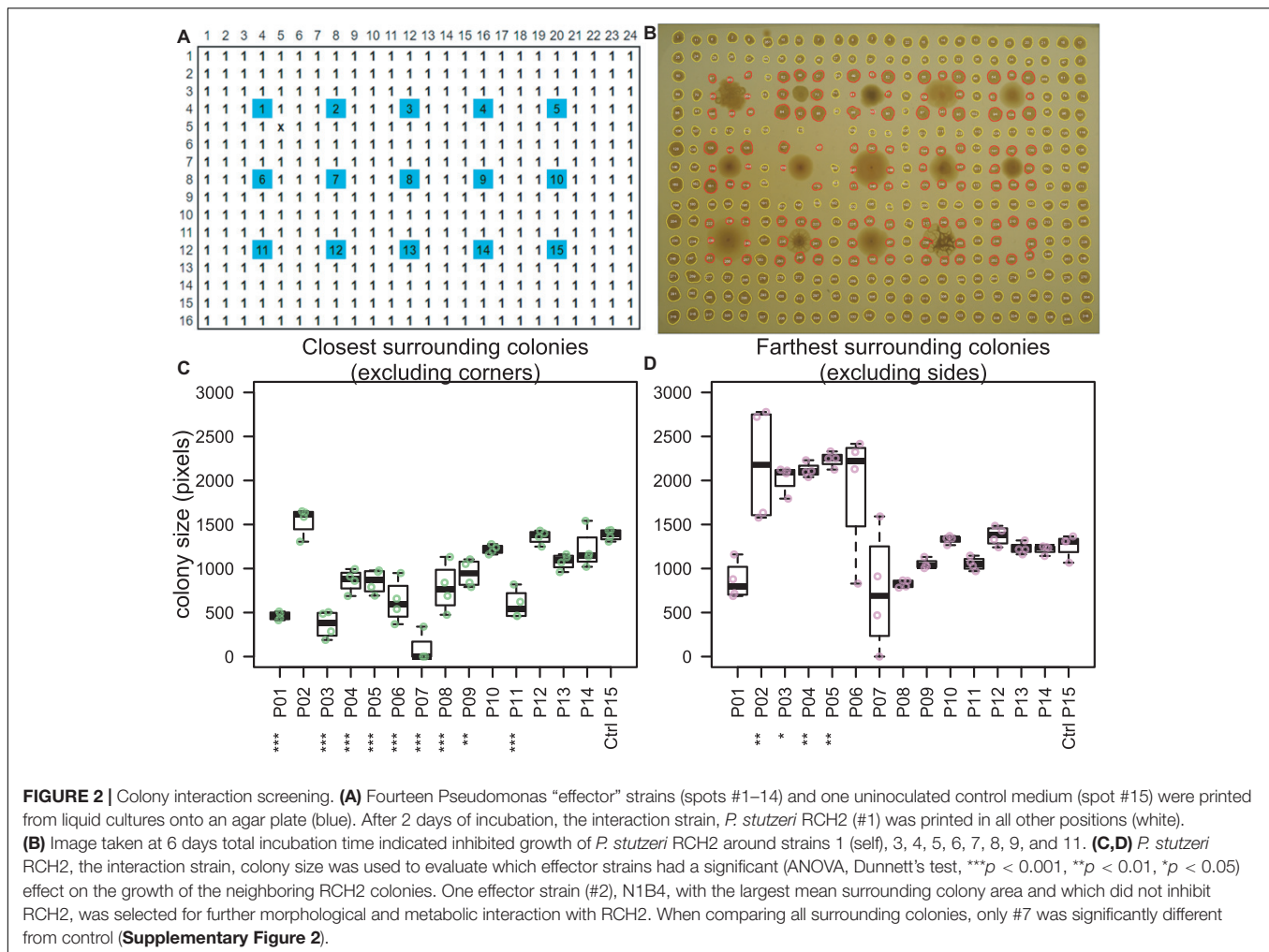
macroscopic morphology, the rim of the petri dish was sealed with parafilm and placed on a black velvet cloth under a Leica M165FC microscope with a Planapo 1.0× objective lens. Images were acquired every 2 min for a 24 h period with a Leica DFC400 1.4 megapixel ccd sensor digital camera set at a 9 mm frame width. For microscopic colony interface analysis, after overnight growth of the overlay, the colony and underlying agar was cut out from the plate and fixed for 2 h with 2.5% glutaraldehyde in 0.1 M sodium cacodylate buffer (pH 7.2). Fixed samples were stained with 5 mM ruthenium red in 0.1 M sodium cacodylate buffer (pH 7.2) for 1 h and post-fixed with 1% osmium tetroxide for 1 h. Following staining, samples were dehydrated through a graded ethanol series (20, 40, 60, 80, 90, 100, 100, and 100%) followed by infiltration with an Embed-812 epoxy resin (Electron Microscopy Sciences):acetone series of 1:3 for 2 h, 2:3 for 2 h, and 100% resin overnight. Samples were then heat polymerized in 100% resin with N,N-dimethylbenzylamine accelerant for 2 h at 85°C. 100 nm sections were cut and sectioned using a Leica UC6 Ultra Microtome (Leica Microsystems Inc., Buffalo Grove, IL, United States) and then stained sequentially with 2% methanolic uranyl acetate and Reynolds' lead citrate for 5 min each. Images were collected using a FEI Tecnai 12 transmission electron microscope (FEI Company, Hillsboro, OR, United States).

Fitness Profiling of RCH2 Mutants in the Presence of Other Pseudomonads

The construction of the *P. stutzeri* RCH2 DNA-barcoded transposon mutant was previously described (Wetmore et al., 2015). Overnight culture of *Pseudomonas* sp. FW300-N1B4 was manually pipetted (10 µL) in triplicate onto LB agar plates. The plates were incubated overnight and then 5 µL of the *P. stutzeri* RCH2 barcoded transposon mutant library (in LB media) starter culture at an OD₆₀₀ of 0.9 was spotted as overlay colonies on top of the three replicates of the underlay colonies. An aliquot of the starter culture was used for the initial RCH2 mutant abundances. Colonies were then carefully scraped and frozen for storage and subsequent analysis of the final *P. stutzeri* RCH2 mutant abundances. Gene fitness scores were calculated by comparing the initial and final mutant abundances as determined by deep sequencing of the DNA barcodes, as previously described (Wetmore et al., 2015).

Mutant Construction

The four mutants from the pooled fitness assay with the largest absolute differential fitness where fitness of RCH2 with N1B4 was less than fitness of RCH2 on agar alone were selected for constructing gene deletion mutant strains. Deletion mutants (**Supplementary Table 2**) for gamma-glutamyl phosphate reductase, OHCU decarboxylase, formyltetrahydrofolate deformylase, and glutamate 5-kinase were constructed by conjugation of unstable, marker-exchange plasmids into *P. stutzeri* RCH2, as previously described (Vaccaro et al., 2016) with modifications as follows. All plasmids and primers (IDT, Newark, NJ) used are listed in **Supplementary Tables 3, 4**, respectively. Briefly, deletion cassettes, containing kanamycin resistance gene (npt) flanked by chromosomal regions up and



downstream of the gene to be deleted, were assembled using the “gene SOEing” technique (Horton et al., 1990). Cloned homologous regions were sequenced at the DNA core facility at the University of Missouri, Columbia, and compared with the published sequence for *P. stutzeri* RCH2 (Chakraborty et al., 2017). Cassettes and the template plasmid pM07704 were amplified by polymerase chain reaction (PCR) with Herculase II DNA polymerase (Stratagene). Marker-exchange plasmids were generated by ligation of the PCR products in α -select cells (Biolone) using the SLIC cloning method (Li and Elledge, 2007). The plasmids were isolated and transformed into *E. coli* strain WM3064, and then transferred to RCH2 via conjugation (Fels et al., 2013). The plasmids, containing up/downstream chromosomal regions flanking *npt*, allow for exchange of *npt* with the gene of interest in RCH2 via double homologous recombination. Exconjugates were selected on 50 $\mu\text{g}/\text{mL}$ kanamycin solid medium, then screened for spectinomycin (100 $\mu\text{g}/\text{mL}$) sensitivity to ensure no single recombination isolates were selected. Deletion strains were confirmed by Southern blot analysis. One isolate for each deletion of interest was retained while the other isolates were discarded. All strains were frozen as early stationary phase cultures in 10% (v/v)

glycerol. RCH2 mutants used for experiments were maintained in Mb-CYM broth or Mb-CYM agar with 50 $\mu\text{g}/\text{mL}$ kanamycin sulfate; kanamycin was not included in subsequent cultures for metabolomics analysis.

Mutant Co-colony Morphology Analysis

Overnight cultures of RCH2 (wild-type and mutants) and N1B4 (500 μL) were centrifuged (5,000 $\times g \times 3$ min at RT) to collect cells, then washed 2 times in DPBS (resuspension in 500 μL DPBS, centrifugation at 5,000 $\times g \times 3$ min at RT) with final resuspension adjusted to an OD (600 nm, 1 cm) of 0.5. Uninoculated control medium was washed and resuspended in a similar manner to account for carryover of nutrients from tube surfaces and residual volumes. Cultures (“underlays”) were manually spotted (2 μL) onto Mb-CYM agar plates in a 7 \times 7 format and incubated overnight at 30°C. Fresh cultures were inoculated from agar stock plates into Mb-CYM. Overlay colonies were diluted and washed in the same manner as for the underlays and then carefully spotted on top of the underlay colonies. Images were taken using a digital camera of whole plates and through a LEICA M165 FC stereo microscope (2x objective) at 24 h (0 h of overlays),

48 h (24 h of overlays), 72 h (48 h of overlays). Morphological differences were visually evaluated.

Metabolomics Analysis

Wild-type and mutant strains of *P. stutzeri* RCH2 were cultured in “spent” N1B4 medium (sterile filtered N1B4 culture supernatant) in liquid culture and then exometabolites were collected by extraction in methanol (Want et al., 2006; Baran et al., 2013; Sitnikov et al., 2016) for LCMS analysis. For collection of “spent” medium, overnight liquid cultures of RCH2 wild-type, RCH2 mutants, and N1B4 wild-type and uninoculated control medium were centrifuged ($3,000 \times g \times 10$ min) to pellet cells. Supernatants were sterile filtered ($0.22 \mu\text{m}$), supplemented with 1x Wolfe’s vitamins and minerals (ATCC) and stored at 4°C overnight. Additional overnight cultures were diluted, washed and adjusted as described above for mutant co-colony morphology analysis, except the final OD was adjusted to 0.12 in DPBS, $20 \mu\text{L}$ of which was added to $100 \mu\text{L}$ of spent medium in 96 well plates. Cultures were prepared in triplicates for all combinations of mutants and wild-type RCH2 on spent N1B4 and fresh Mb-CYM and for N1B4 on all combinations of spent mutants and wild-type RCH2 and fresh Mb-CYM; uninoculated controls were included for each spent medium and positive growth controls were included for each strain on fresh (non-spent) medium. Cultures were incubated for 20 h in a BioTek plate reader with OD readings taken every 30 min at 600 nm . Cross-feeding medium from the culture was then collected via centrifugation ($3,000 \times g$ for 5 min), transferred to a new plate that was sealed with heated foil (4titude), and frozen at -80°C . Holes were pierced in the foil with an 18 gauge needle and then supernatants were lyophilized to dryness. Dried material was resuspended in $200 \mu\text{L}$ of internal standard mix ($15 \mu\text{M}$ 13C, 15N amino acid mix, $10 \mu\text{g}/\text{mL}$ 13C-mannitol, 13C-trehalose and $2 \mu\text{M}$ 15N4-inosine, 15N5-adenine, 13C4-15N2-uracil, 15N4-hypoxanthine, 13C4-15N2-thymine) in LCMS grade methanol, resealed, vortexed, sonicated in a room temperature water bath for 10 min, rechilled at -80°C for 5 min, and centrifuged $3,000 \times g$ for 5 min to pellet insoluble material. Supernatants were filtered ($0.22 \mu\text{m}$, PVDF) using an Apricot positive pressure filtration device. Filtrates were then arrayed into $50 \mu\text{L}$ aliquots in a 384 well plate for LCMS analysis.

LCMS Analysis of Exometabolites From Spent Media Fed Cultures

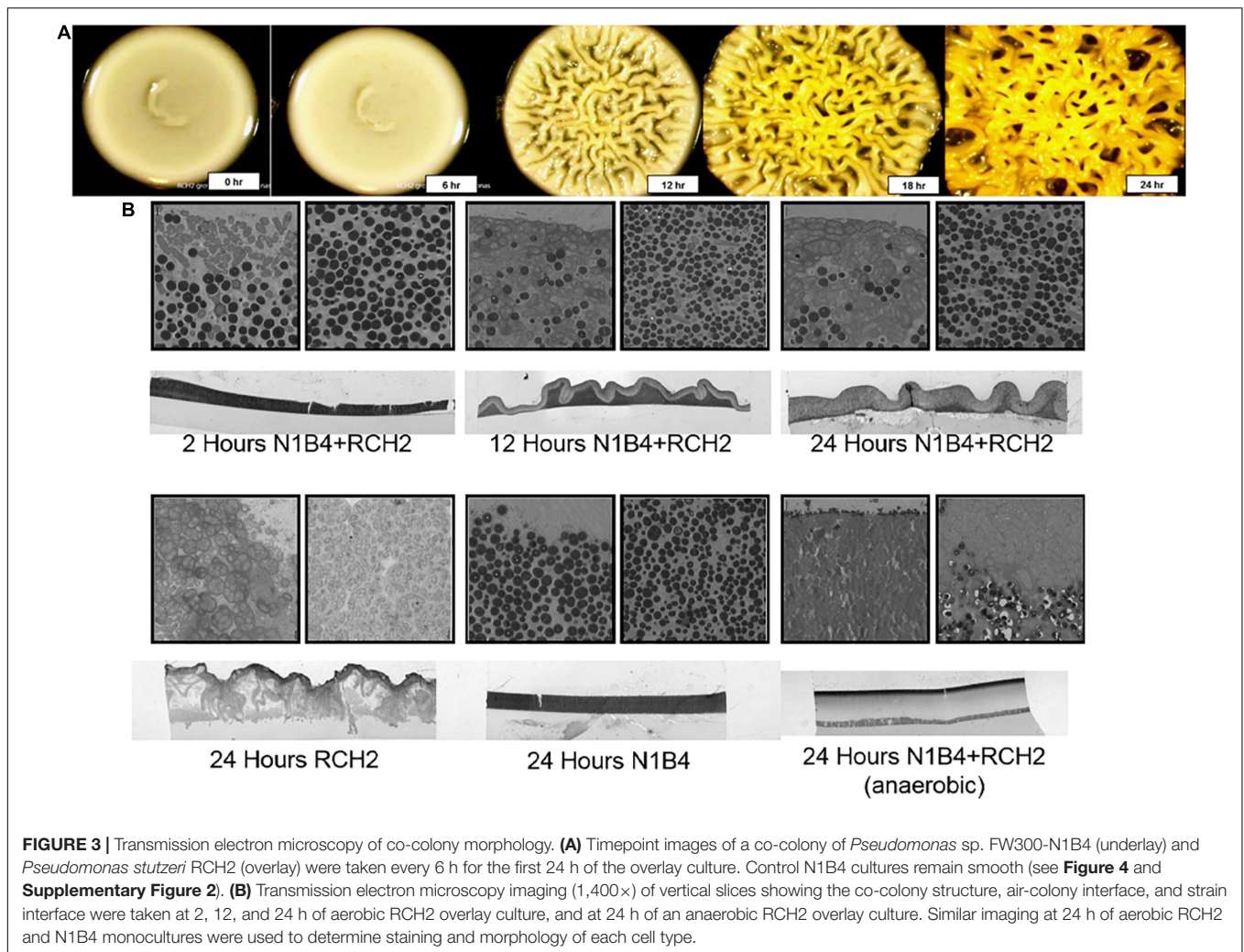
Extracts of polar metabolites were analyzed using hydrophilic interaction chromatography—mass spectrometry. Metabolites were retained and separated on an InfinityLab Poroshell 120 HILIC-Z column (Agilent, 683775-924, $2.7 \mu\text{m}$, $150 \times 2.1 \text{ mm}$) using an Agilent 1290 UHPLC. Samples, held at 4°C , were injected at $4 \mu\text{L}$ each; the column temperature was held at 40°C and flow rate was held at a constant $0.45 \text{ mL}/\text{min}$. Following injection, a gradient of mobile phase A (5 mM ammonium acetate, 0.2% acetic acid, 5 μM methylene di-phosphonic acid in water) and mobile phase B [5 mM ammonium acetate, 0.2% acetic acid in 95:5 (v/v) acetonitrile:water] was applied as follows: initial equilibration at 100% B for 1.0 min, linear decrease to

89% B over 10 min, linear decrease to 70% B over 4.75 min, linear decrease to 20% B over 0.5 min, hold at 20% B for 2.25 min, linear increase to 100% B over 0.1 min, re-equilibration at 100% B for 2.4 min. Eluted metabolites were subjected to mass spectrometry analysis on a Q Exactive Hybrid Quadrupole-Orbitrap Mass Spectrometer (Thermo Fisher Scientific) equipped with a HESI-II source probe using Full MS with Data Dependent tandem MS. Source settings were as follows: sheath gas at 55 (arbitrary units), aux gas flow at 20, sweep gas at 2, spray voltage at $3 | \text{kV} |$ spray, capillary temperature at 400°C , and S-lens RF at 50. MS1 was set at 70,000 mass resolution, with automatic gain control target at $3.0\text{E}06$ with a maximum allowed injection time of 100 ms, at a $70\text{--}1,050 \text{ m}/\text{z}$ scan range. dd-MS2 was set at 17,500 mass resolution with automatic gain control target at $1.0\text{E}5$ and a maximum allowed injection time of 50 ms, a $2 \text{ m}/\text{z}$ isolation window and stepped normalized collision energies at 10, 20, and 30 (dimensionless units). All data was collected in centroid mode. The scan cycle included a single MS1 scan followed by sequential MS/MS of the top two most intense MS1 ions excluding any fragmented within the previous 10 s. Ions selected for fragmentation must meet a minimum AGC target threshold of $1.0\text{E}3$ with absolute charge less than four. Each sample was analyzed in negative ionization mode. Sample were injected in randomized order with solvent blank injections between each; internal and external standards were used for quality control purposes and for retention time predictions of compounds from in an in-house standards library. Using custom python scripts and metabolite atlases (Bowen and Northen, 2010; Yao et al., 2015), mass-to-charge ratios, retention times and where possible spectra fragmentation patterns were used to confirm metabolite identification by comparison to metabolite standards analyzed using the same LC-MS/MS methods. Mutant and RCH2 cultures on N1B4 medium were compared with uninoculated control N1B4 spent medium using ANOVA and Tukey HSD in R.

RESULTS

Biofilm Interaction Mapping and Analysis Screening: Microbial Interaction Mapping and Strain Selection

As the first step of BIMA, a colony printing method was developed on an automated liquid handling system for the purpose of scalability and transferability between labs. Fourteen preprinted “effector” *Pseudomonas* strains (including RCH2) were evaluated for their effect on the growth of subsequently printed neighboring colonies of *P. stutzeri* RCH2 (Figures 2A,B). *Pseudomonas* strains 3–9, and 11 inhibited the growth of the four closest RCH2 colonies, located along the sides of the square of neighboring colonies (Figure 2C). Interestingly, for a subset of these (3, 4, 5), the more distant RCH2 colonies at the corners of the square of neighboring colonies had larger mean areas (Figure 2D). *Pseudomonas* strain 2 (*Pseudomonas fluorescens* FW300-N1B4) was the only strain that did not inhibit RCH2 (closest side colonies) and



enhanced the growth of RCH2 (corner colonies). This strain “N1B4,” was selected for further analysis in co-culture with *P. stutzeri* RCH2.

Biofilm Interaction Mapping and Analysis Morphology: Co-colony Structure and Infiltration

Time lapse images of the RCH2 overlay on N1B4 were taken to evaluate the co-colony morphology. Highly wrinkled, rugose colony morphology had formed by 12 h after application of the RCH2 overlay (**Figure 3A**). The co-colony species interface was further examined using transmission electron microscopy (TEM) (**Figure 3B**). TEM after 2 h showed a stratification with a clear distinction between RCH2 on the surface and N1B4 underneath. Over the course of 24 h, the colonies became more mixed with infiltration of the N1B4 layer by RCH2. In both the co-culture and in isolate culture, RCH2 biofilm developed sacs containing groups of spherical cells at the air interface; whereas when spotted on the surface of N1B4, single, elongated RCH2 are observed at the N1B4 interface. The sacs became visible in the 24 h co-colony.

The anaerobic co-colony culture developed a compact RCH2 layer with no visible EPS sacs.

Biofilm Interaction Mapping and Analysis Genomics: Mutant Fitness Analysis and Interactions

A pooled mutant fitness assay was used to identify RCH2 genes essential for successful aerobic co-culture growth with N1B4; the anaerobic culture was not evaluated further since no morphological interaction was observed. The top four genes with the largest differential gene fitness between RCH2 on LB and RCH2 on N1B4, where fitness on N1B4 was negative included gamma-glutamyl phosphate reductase (*proA*), OHCU decarboxylase (*uraD*), formyltetrahydrofolate deformylase (*purU*), and glutamate 5-kinase (*proB*) (**Figure 4A**). To investigate these genes further, we constructed isogenic single-gene deletion strains for all four genes.

In liquid culture, while all mutants were capable of growth on fresh medium, only the Δ *uraD* deletion strain had similar growth to the wild-type when cultured on spent N1B4 medium

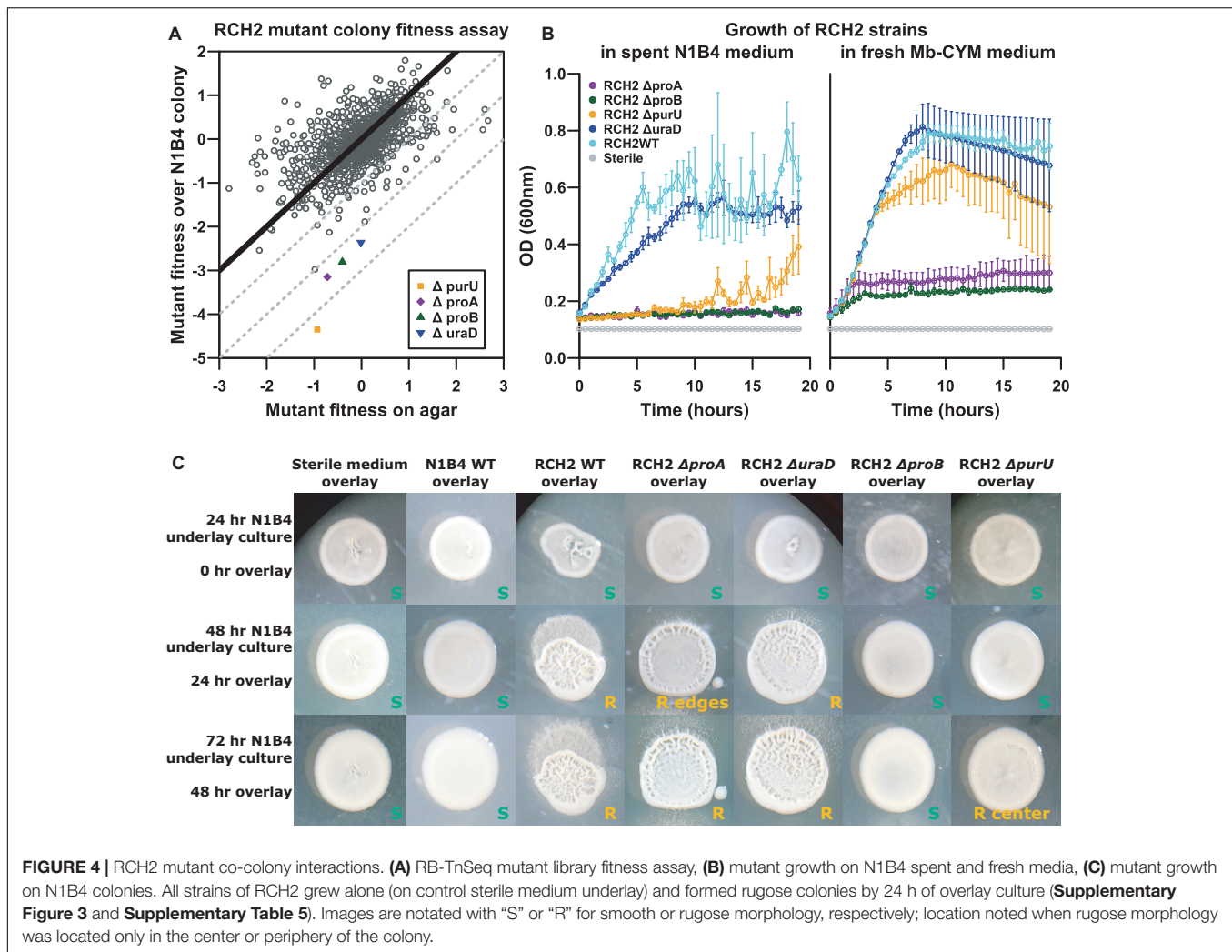
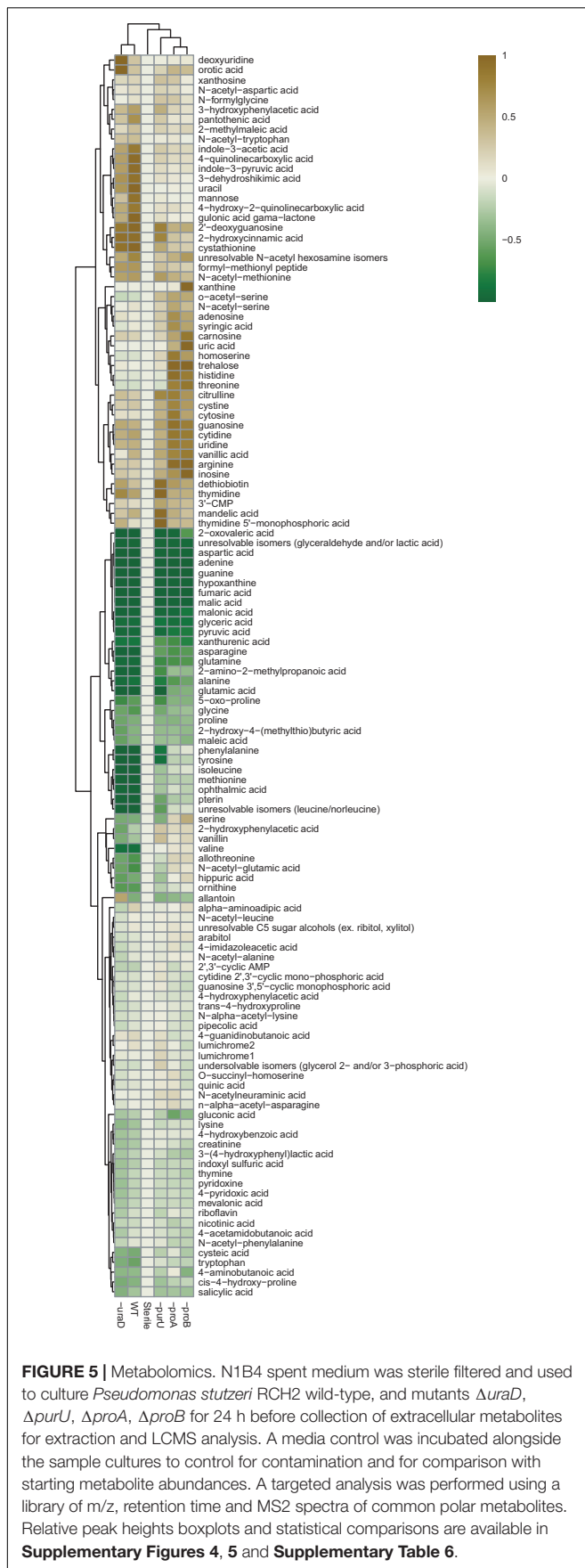


(Figure 4B). Minimal to no growth was observed for the $\Delta proA$ and $\Delta proB$ deletion mutants, and delayed growth was observed for the $\Delta purU$ deletion mutant. N1B4 had similar growth on the spent medium of RCH2 wild-type and mutants (not shown). The limited or delayed growth indicated these mutants were unable to acquire some required metabolite from the medium that was consumed by N1B4 in liquid culture or that growth may have been inhibited by something N1B4 was producing.

The biofilm interactions were analyzed by manual printing of the RCH2 wild-type and mutant strains on the top of an established N1B4 colony. The overlays were imaged at 24 and 48 h after overlay printing (Figure 4C). Wild-type RCH2, and $\Delta proA$ and $\Delta uraD$ deletion strains formed rugose co-colony biofilms after 24 h similar to the wild-type but with a smoother center for $\Delta proA$, while the $\Delta purU$ mutant had delayed rugose formation and the $\Delta proB$ mutant remained smooth up to 72 h of observation. All mutants formed rugose colonies after 24 h of overlay on control medium. On its own, the $\Delta purU$ formed more tubular structures than the wild-type alone, similar to growth on N1B4 for both (Supplementary Figure 3).

Biofilm Interaction Mapping and Analysis Exometabolomics: Potential for Metabolite Exchange

To further evaluate why the four RCH2 genes identified in the mutant fitness assay were important to growth in the aerobic co-colony, spent medium from N1B4 was fed to each of the mutants described above and the wild-type RCH2 and then metabolomics was performed to check for altered metabolism in the mutants. Despite limited growth of three of the mutants on N1B4 spent medium (Figure 4B), all four RCH2 mutants appeared to be metabolically active with significant increases and decreases in metabolite abundances relative to uninoculated N1B4 spent medium. In many cases the changes were significantly different than the wild-type (Figure 5 and Supplementary Figures 4, 5). The *P. stutzeri* RCH2 wildtype consumed several N1B4 metabolites involved in one-carbon (C1) metabolism though consumption of methionine was reduced in *P. stutzeri* RCH2 strain JWST9066 ($\Delta purU$) (Supplementary Figure 5). *P. stutzeri* RCH2 strain JWST9063 ($\Delta uraD$) accumulated allantoin, presumably from spontaneous



conversion of 2-oxo-4-hydroxy-4-carboxy-5-ureidoimidazole (OHCU) to (R)-allantoin. *P. stutzeri* RCH2 strain JWST9060 ($\Delta proA$) and *P. stutzeri* RCH2 strain JWST9069 ($\Delta proB$), had reduced consumption of glutamate (precursor in proline synthesis) from N1B4, when compared to wild-type, and similar consumption of proline (**Supplementary Figure 5**).

DISCUSSION

Biofilm formation and morphology in pseudomonas appears to be regulated by a combination of biotic factors including, but not limited to: phenazines, exopolysaccharide production, signaling molecules and flagellar activity (Merritt et al., 2010). In pigmented species of pseudomonas, it has been shown that a reduced cytoplasm (induced under anoxic and low nitrate conditions) as measured by NADH:NAD + ratio results in a rugose or wrinkled colony morphology while under aerobic and normal nitrate conditions, where reduction of phenazines or nitrate to dinitrogen gas occurs, they maintain a smooth morphology (Dietrich et al., 2013). Interestingly, *P. stutzeri*, has a distinguishing morphological characteristic of forming rugose or wrinkled colonies following initial isolation and culture on agar. While brown in color due to cytochrome c, they are classified as a non-pigmented, non-fluorescent pseudomonas and are not known to produce phenazines (Lalucat et al., 2006). *P. stutzeri* can grow anaerobically in the presence of nitrate and has been used for denitrification purposes (Lalucat et al., 2006). However, it has been demonstrated that after repeated culture, smooth colonies can form and it may take several transfers in nitrate media under semi-aerobic conditions before they are able to grow under denitrifying anaerobic conditions (Lalucat et al., 2006).

Using BIMA, we were able to screen colony forming microbial effector strains for growth promoting and inhibiting effects on *P. stutzeri*. TEM imaging revealed unique cellular morphologies of the *P. stutzeri* RCH2 on the surface of *P. fluorescens* FW300-N1B4. In other *P. stutzeri* strains, exopolysaccharide sacs have been shown to be associated with oxygen exclusion for nitrogen fixation under aerobic conditions (Wang et al., 2017). However, we observed a loss of sac formation at the species interface, suggesting possible exchange of nitrogen containing compounds from N1B4 to RCH2 obviating the need for nitrogen fixation. We observed that N1B4 metabolites supported the growth of RCH2 and metabolomics analysis confirmed consumption of its metabolites. The mutant analysis provided further support for this view. Specifically, we saw that the $\Delta purU$ mutant's consumption of metabolites was altered and its growth was inhibited. Given that PurU is important in maintenance of one carbon pools, the $\Delta purU$ mutant may be unable to obtain the reaction products (THF and formate) from N1B4, and as suggested by previous studies in *E. coli*, may experience glycine starvation due to GlyA inhibition by methionine and adenine (Nagy et al., 1995), both metabolites RCH2 took up from N1B4 based media. In the $\Delta uraD$ mutant, which accumulated allantoin, presumably (R)-allantoin, RCH2 would be unable to use this in downstream nitrogen assimilation pathways without a racemase (Bovigny et al., 2014), an enzyme *P. stutzeri* has been shown to lack (Van Der Drift et al., 1975). Thus UraD is probably essential for converting OHCU into usable (S)-allantoin. In some

bacterial species, the ureide pathway is utilized for recovery of nitrogen from purines under stress conditions (Serventi et al., 2010; Izaguirre-Mayoral et al., 2018). Under aerobic conditions or presence of ammonia, N₂ fixation in *P. stutzeri* is suppressed and nitrification is active, however, in biofilm, nitrogen fixation is suspected to occur in the EPS sacs produced by the rugose morphology (Yan et al., 2010; Wang et al., 2017). At the N1B4—RCH2 interface of the co-colony (which lacked EPS sacs in imaging) and in liquid culture with shaking and sufficient gas exchange, nitrogen fixation may be suppressed in favor of utilization of exchanged organic nitrogen compounds such as intermediate allantoin precursors (5-hydroxyisouric acid or OHCU) from N1B4 spent medium, prior to conversion to usable (S)-allantoin. With the $\Delta proA$ and the $\Delta proB$ mutants, both known auxotrophs for proline,¹ we observed that while proline was still consumed, glutamate was not to the same extent as wildtype. The wild-type may use exchanged glutamate for proline synthesis while the proline synthesis mutants are likely unable to obtain enough proline directly from N1B4 and is likely unable to sufficiently utilize alternative sources such peptide degradation or by alternative synthesis from ornithine (Supplementary Figure 5). Together, these results indicate the growth of the RCH2 may be reliant upon uptake of metabolites produced by the N1B4.

While our experiments focused on cooperative interactions, inhibitory interactions may be of interest in controlling pathogenic strains in agricultural systems. The inhibitory interactions of certain pseudomonas species have been studied in detail. For example, some pathogenic species of pseudomonads produce lipodepsipeptides (e.g., corpeptins from *P. corrugata*, a plant pathogen) which also have antimicrobial activity (Raaijmakers et al., 2010). These may contribute to interspecific competition between pseudomonads by inhibiting biofilm formation and breaking down existing biofilm (Kuiper et al., 2004). An interesting follow up study involving a mutant library of *Pseudomonas corrugate* N2F2, may elucidate the mechanism of inhibition between the two species and the nature of its competitive and pathogenic behavior in nature. Additionally, some beneficial strains such as *P. aureofaciens*, an anti-fungal symbiont of wheat, releases phenazines in the rhizosphere which inhibit the growth of plant pathogens in response to exogenously diffusible signaling molecules (Pierson and Pierson, 1996). These compounds may contribute to competitiveness and the ability to form biofilms (Ramos et al., 2010). Interestingly, phenazines may have multiple functional roles (Mavrodi et al., 2006), including involvement of the redox state of the cytoplasm (Dietrich et al., 2013; Glasser et al., 2014); interactions such as these may be important determinants of co-colony biofilm structure under varying oxygenic conditions.

In this proof of concept study, we focused on existing isolates in co-culture studied under ideal lab growth conditions. We recognize the importance of extending this method in future work to more diverse isolates representing the field microbiome. However, community studies present additional challenges in determining metabolic functions associated with

specific microbes. Further, in using BIMA to uncover more environmentally relevant metabolic activities, growth conditions should represent environmental parameters as closely as possible (for example, the use of soil extract, soil based synthetic medium or sterilized soil for microbial growth) (Jenkins et al., 2017; Swenson et al., 2018). The development of ecologically relevant media based on analysis of soil and sediment metabolites is an important future direction for increasing the ecological relevance of these microbial interaction studies. Analytical methods for metabolite extraction and detection should be selected to ensure proper coverage of metabolites of interest (Mushtaq et al., 2014; Louie et al., 2020).

In this work we have demonstrated that bacterial printing can be used to rapidly screen for macroscopic interactions such as changes to colony morphology, size and color. We take advantage of a mutant fitness library and metabolomics to gain insights into genes and compounds mediating observed bacterial interactions. We anticipate that this approach integrating bacterial printing, mutant fitness libraries, targeted genetics, and metabolomics is suitable to investigating diverse microbial interactions. In some instances, cooperative growth may be favorable (such as for bioremediation purposes where both consortia and biofilm-based systems are used). In other cases, competitive interactions may be desired for biocontrol-based purposes or for understanding competitive interactions in soil environments. Knowledge of the genomic and metabolic determinants involved in these interactions allows for more directed design of co-colony-based systems and a better understanding of those existing in nature. We foresee BIMA becoming a valuable tool for the enhancement and understanding of *P. stutzeri* and other co-colony-based systems.

DATA AVAILABILITY STATEMENT

Raw LCMS data are available from the JGI Genome Portal² under project number 1278333.

AUTHOR CONTRIBUTIONS

SK, PR, and TN wrote the manuscript. SK, PR, KW, MZ, GZ, MA, and JZ performed the experiments. SK and BB performed data analysis. MR made revisions. RC maintained and provided bacterial strains. JW, AA, AD, and TN oversaw study and made critical revisions. All authors reviewed and approved the manuscript.

FUNDING

Study design, sample collection, data analysis and interpretation, and manuscript preparation by ENIGMA (Ecosystems and Networks Integrated with Genes and Molecular Assemblies, <http://enigma.lbl.gov>, a Scientific Focus Area Program at Lawrence Berkeley National Laboratory), is supported by the

¹<http://fit.genomics.lbl.gov/> (accessed 05/14/2020).

²genome.jgi.doe.gov

U.S. Department of Energy, Office of Science, Office of Biological and Environmental Research, Genomic Sciences Program under contract number DE-AC02-05CH11231 to Lawrence Berkeley National Laboratory. Data analysis used resources of the National Energy Research Scientific Computing Center, a Department of Energy Office of Science User Facility operated under contract number DE-AC02-05CH11231. The funders had no role in study design, data collection and interpretation, or the decision to submit the work for publication.

REFERENCES

- Badar, U., Shoeb, E., Qureshi, F. M., Akhtar, J., and Ahmed, N. (2013). Removal of copper via bioreactor by soil isolate. *Acad. Res. Int.* 4, 253–259.
- Baran, R., Bowen, B. P., Price, M. N., Arkin, A. P., Deutschbauer, A. M., and Northen, T. R. (2013). Metabolic footprinting of mutant libraries to map metabolite utilization to genotype. *ACS Chem. Biol.* 8, 189–199. doi: 10.1021/cb300477w
- Baran, R., Reindl, W., and Northen, T. R. (2009). Mass spectrometry based metabolomics and enzymatic assays for functional genomics. *Curr. Opin. Microbiol.* 12, 547–552. doi: 10.1016/j.mib.2009.07.004
- Bovigny, C., Degiacomi, M. T., Lemmin, T., Dal Peraro, M., and Stenta, M. (2014). Reaction mechanism and catalytic fingerprint of allantoin racemase. *J. Phys. Chem. B* 118, 7457–7466. doi: 10.1021/jp411786z
- Bowen, B. P., and Northen, T. R. (2010). Dealing with the unknown: metabolomics and metabolite atlases. *J. Am. Soc. Mass Spectrom.* 21, 1471–1476. doi: 10.1016/j.jasms.2010.04.003
- Brodie, E. L., Joyner, D. C., Faybishenko, B., Conrad, M. E., Rios-Velazquez, C., Malave, J., et al. (2011). Microbial community response to addition of polylactate compounds to stimulate hexavalent chromium reduction in groundwater. *Chemosphere* 85, 660–665. doi: 10.1016/j.chemosphere.2011.07.021
- Chakraborty, R., Woo, H., Dehal, P., Walker, R., Zemla, M., Auer, M., et al. (2017). Complete genome sequence of *Pseudomonas stutzeri* strain RCH2 isolated from a Hexavalent Chromium [Cr(VI)] contaminated site. *Stand. Genomic Sci.* 12:23. doi: 10.1186/s40793-017-0233-7
- Clarens, M., Bernet, N., Delgenès, J. P., and Moletta, R. (1998). Effects of nitrogen oxides and denitrification by *Pseudomonas stutzeri* on acetotrophic methanogenesis by *Methanosarcina mazei*. *FEMS Microbiol. Ecol.* 25, 271–276. doi: 10.1016/S0168-6496(98)00008-7
- Cottyn, B., Debode, J., Regalado, E., Mew, T. W., and Swings, J. (2009). Phenotypic and genetic diversity of rice seed-associated bacteria and their role in pathogenicity and biological control. *J. Appl. Microbiol.* 107, 885–897. doi: 10.1111/j.1365-2672.2009.04268.x
- Deng, B., Fu, L., Zhang, X., Zheng, J., Peng, L., Sun, J., et al. (2014). The denitrification characteristics of *Pseudomonas stutzeri* SC221-M and its application to water quality control in grass carp aquaculture. *PLoS One* 9:e114886. doi: 10.1371/journal.pone.0114886
- Dietrich, L. E. P., Okegbe, C., Price-Whelan, A., Sakhtah, H., Hunter, R. C., and Newman, D. K. (2013). Bacterial community morphogenesis is intimately linked to the intracellular redox state. *J. Bacteriol.* 195, 1371–1380. doi: 10.1128/JB.02273-12
- Erna, N. M., Banerjee, S., Khatoon, H., Shariff, M., and Yusoff, F. M. D. (2013). Immobilized nitrifying bacterial consortium for improving water quality, survival and Growth of *Panaeus monodon* Fabricius 1798 Postlarvae in Hatchery System. *Asian Fish. Sci.* 26, 212–221.
- Fels, S. R., Zane, G. M., Blake, S. M., and Wall, J. D. (2013). Rapid transposon liquid enrichment sequencing (TnLE-seq) for gene fitness evaluation in underdeveloped bacterial systems. *Appl. Environ. Microbiol.* 79, 7510–7517. doi: 10.1128/AEM.02051-13
- Gałazka, A., Król, M., and Perzyński, A. (2012). The efficiency of rhizosphere bioremediation with *Azospirillum* sp. and *Pseudomonas stutzeri* in soils freshly contaminated with PAHs and diesel fuel. *Pol. J. Environ. Stud.* 21, 345–353.

ACKNOWLEDGMENTS

Preprint of article draft published online (Kosina et al., 2021).

SUPPLEMENTARY MATERIAL

The Supplementary Material for this article can be found online at: <https://www.frontiersin.org/articles/10.3389/fmicb.2021.757856/full#supplementary-material>

- Garbeva, P., Van Veen, J. A., and Van Elsas, J. D. (2004). Assessment of the diversity, and antagonism towards *Rhizoctonia solani* AG3, of *Pseudomonas* species in soil from different agricultural regimes. *FEMS Microbiol. Ecol.* 47, 51–64. doi: 10.1016/S0168-6496(03)00234-4
- Glasser, N. R., Kern, S. E., and Newman, D. K. (2014). Phenazine redox cycling enhances anaerobic survival in *Pseudomonas aeruginosa* by facilitating generation of ATP and a proton-motive force. *Mol. Microbiol.* 92, 399–412. doi: 10.1111/mmi.12566
- Goodman, A. L., Wu, M., and Gordon, J. I. (2011). Identifying microbial fitness determinants by insertion sequencing using genome-wide transposon mutant libraries. *Nat. Protoc.* 6, 1969–1980. doi: 10.1038/nprot.2011.417
- Han, R., Geller, J. T., Yang, L., Brodie, E. L., Chakraborty, R., Larsen, J. T., et al. (2010). Physiological and transcriptional studies of Cr(VI) reduction under aerobic and denitrifying conditions by an aquifer-derived pseudomonad. *Environ. Sci. Technol.* 44, 7491–7497. doi: 10.1021/es101152r
- Han, R., Qin, L., Brown, S. T., Christensen, J. N., and Beller, H. R. (2012). Differential isotopic fractionation during Cr(VI) reduction by an aquifer-derived bacterium under aerobic versus denitrifying conditions. *Appl. Environ. Microbiol.* 78, 2462–2464. doi: 10.1128/AEM.07225-11
- Horton, R. M., Cai, Z. L., Ho, S. N., and Pease, L. R. (1990). Gene splicing by overlap extension: tailor-made genes using the polymerase chain reaction. *Biotechniques* 8, 528–535. doi: 10.2144/000114017
- Hothorn, T., Bretz, F., and Westfall, P. (2008). Simultaneous inference in general parametric models. *Biom. J.* 50, 346–363. doi: 10.1002/bimj.200810425
- Izaguirre-Mayoral, M. L., Lazarovits, G., and Baral, B. (2018). Ureide metabolism in plant-associated bacteria: purine plant-bacteria interactive scenarios under nitrogen deficiency. *Plant Soil* 428, 1–34. doi: 10.1007/s11104-018-3674-x
- Jenkins, S., Swenson, T. L., Lau, R., Rocha, A. M., Aaring, A., Hazen, T. C., et al. (2017). Construction of viable soil defined media using quantitative metabolomics analysis of soil metabolites. *Front. Microbiol.* 8:2618. doi: 10.3389/fmicb.2017.02618
- Jiang, Q., Zhou, C., Wang, Y., Si, F., Zhou, Y., Chen, B., et al. (2014). *Pseudomonas stutzeri* strain possessing a self-transmissible TOL-like plasmid degrades phenol and promotes maize growth in contaminated environments. *Appl. Biochem. Biotechnol.* 172, 3461–3475. doi: 10.1007/s12010-014-0785-6
- Kaczorek, E., Jesionowski, T., Giec, A., and Olszanowski, A. (2012). Cell surface properties of *Pseudomonas*. *Biotechnol. Lett.* 34, 857–862. doi: 10.1007/s10529-011-0835-x
- Kosina, S. M., Danielewicz, M. A., Mohammed, M., Ray, J., Suh, Y., Yilmaz, S., et al. (2016). Exometabolomics assisted design and validation of synthetic obligate mutualism. *ACS Synth. Biol.* 5, 569–576. doi: 10.1021/acssynbio.5b00236
- Kosina, S. M., Rademacher, P., Wetmore, K. M., de Raad, M., Zemla, M., Zane, G. M., et al. (2021). Biofilm interaction mapping and analysis (BIMA): a tool for deconstructing interspecific interactions in co-culture biofilms. *bioRxiv*. doi: 10.1101/2021.08.03.454817
- Kuiper, I., Lagendijk, E. L., Pickford, R., Derrick, J. P., Lamers, G. E. M., Thomas-Oates, J. E., et al. (2004). Characterization of two *Pseudomonas*. *Mol. Microbiol.*, 97–113. doi: 10.1046/j.1365-2958.2003.03751.x
- Lalucat, J., Bennisar, A., Bosch, R., García-Valdés, E., and Palleroni, N. J. (2006). Biology of *Pseudomonas stutzeri*. *Microbiol. Mol. Biol. Rev.* 70, 510–547. doi: 10.1128/MMBR.00047-05

- Lazarova, V. Z., Capdeville, B., and Nikolov, L. (1992). Biofilm performance of a fluidized bed biofilm reactor for drinking water denitrification. *Water Sci. Technol.* 26, 555–566. doi: 10.2166/wst.1992.0435
- Li, L., Abu Al-Soud, W., Bergmark, L., Riber, L., Hansen, L. H., Magid, J., et al. (2013). Investigating the diversity of *Pseudomonas*. *Curr. Microbiol.* 67, 423–430. doi: 10.1007/s00284-013-0382-x
- Li, M. Z., and Elledge, S. J. (2007). Harnessing homologous recombination in vitro to generate recombinant DNA via SLIC. *Nat. Methods* 4, 251–256. doi: 10.1038/nmeth1010
- Liu, D., Zhang, S., Zheng, Y., and Shoun, H. (2006). Denitrification by the mix-culturing of fungi and bacteria with shell. *Microbiol. Res.* 161, 132–137. doi: 10.1016/j.micres.2005.07.002
- Louie, K. B., Bowen, B. P., Cheng, X., Berleman, J. E., Chakraborty, R., Deutschbauer, A., et al. (2013). Replica-Extraction-Transfer” nanostructure-initiator mass spectrometry imaging of acoustically printed bacteria. *Anal. Chem.* 85, 10856–10862. doi: 10.1021/ac402240q
- Louie, K. B., Kosina, S. M., Hu, Y., Otani, H., de Raad, M., Kuffin, A. N., et al. (2020). “Mass spectrometry for natural product discovery,” in *Comprehensive Natural Products III*, eds H.-W. Liu and T. P. Begley (Oxford: Elsevier), 263–306. doi: 10.1016/B978-0-12-409547-2.14834-6
- Mavrodi, D. V., Blankenfeldt, W., and Thomashow, L. S. (2006). Phenazine compounds in fluorescent *Pseudomonas* spp. biosynthesis and regulation. *Annu. Rev. Phytopathol.* 44, 417–445. doi: 10.1146/annurev.phyto.44.013106.145710
- Merritt, J. H., Ha, D. G., Cowles, K. N., Lu, W., Morales, D. K., Rabinowitz, J., et al. (2010). Specific control of *Pseudomonas aeruginosa* surface-associated behaviors by two c-di-GMP diguanylate cyclases. *mBio* 1:e00183-10. doi: 10.1128/mBio.00183-10
- Miyahara, M., Kim, S.-W., Zhou, S., Fushinobu, S., Yamada, T., Ikeda-Ohtsubo, W., et al. (2012). Survival of the aerobic denitrifier *Pseudomonas stutzeri* Strain TR2 during co-culture with activated sludge under denitrifying conditions. *Biosci. Biotechnol. Biochem.* 76, 495–500. doi: 10.1271/bbb.110785
- Moore, E. R. B., Tindall, B. J., Martins Dos, Santos, V. A. P., Pieper, D. H., Ramos, J.-L., et al. (2006). “Nonmedical: *Pseudomonas*,” in *The Prokaryotes: A Handbook on the Biology of Bacteria Volume 6: Proteobacteria: Gamma Subclass*, eds M. Dworkin, S. Falkow, E. Rosenberg, K.-H. Schleifer, and E. Stackebrandt (New York, NY: Springer), 646–703. doi: 10.1007/0-387-30746-X_21
- Moscato, F., Deive, F. J., Longo, M. A., and Sanromán, M. A. (2012a). Technoeconomic assessment of phenanthrene degradation by *Pseudomonas stutzeri* CECT 930 in a batch bioreactor. *Bioresour. Technol.* 104, 81–89. doi: 10.1016/j.biortech.2011.10.053
- Moscato, F., Deive, F. J., Villar, P., Pena, R., Herrero, L., Longo, M. A., et al. (2012b). Assessment of a process to degrade metal working fluids using *Pseudomonas stutzeri* CECT 930 and indigenous microbial consortia. *Chemosphere* 86, 420–426. doi: 10.1016/j.chemosphere.2011.10.012
- Mushtaq, M. Y., Choi, Y. H., Verpoorte, R., and Wilson, E. G. (2014). Extraction for metabolomics: access to the metabolome. *Phytochem. Anal.* 25, 291–306. doi: 10.1002/pca.2505
- Nagy, P. L., Marolewski, A., Benkovic, S. J., and Zalkin, H. (1995). Formyltetrahydrofolate hydrolase, a regulatory enzyme that functions to balance pools of tetrahydrofolate and one-carbon tetrahydrofolate adducts in *Escherichia coli*. *J. Bacteriol.* 177, 1292–1298. doi: 10.1128/jb.177.5.1292-1298.1995
- Nguyen, P. D., Van Ginkel, C. G., and Plugge, C. M. (2008). Anaerobic degradation of long-chain alkylamines by a denitrifying *Pseudomonas stutzeri*. *FEMS Microbiol. Ecol.* 66, 136–142. doi: 10.1111/j.1574-6941.2008.00564.x
- Peix, A., Ramírez-Bahena, M. H., and Velázquez, E. (2009). Historical evolution and current status of the taxonomy of genus *Pseudomonas*. *Infect. Genet. Evol.* 9, 1132–1147. doi: 10.1016/j.meegid.2009.08.001
- Pierson, L. S., and Pierson, E. A. (1996). Phenazine antibiotic production in *Pseudomonas aureofaciens*: role in rhizosphere ecology and pathogen suppression. *FEMS Microbiol. Lett.* 136, 101–108. doi: 10.1016/0378-1097(95)00489-0
- Price, M. N., Wetmore, K. M., Waters, R. J., Callaghan, M., Ray, J., Liu, H., et al. (2018). Mutant phenotypes for thousands of bacterial genes of unknown function. *Nature* 557, 503–509. doi: 10.1038/s41586-018-0124-0
- R Core Team (2014). *R: A Language and Environment for Statistical Computing*. Vienna: R Foundation for Statistical Computing.
- Raaijmakers, J. M., de Bruijn, I., Nybroe, O., and Ongena, M. (2010). Natural functions of lipopeptides from *Bacillus* and *Pseudomonas*: more than surfactants and antibiotics. *FEMS Microbiol. Rev.* 34, 1037–1062. doi: 10.1111/j.1574-6976.2010.00221.x
- Ramos, I., Dietrich, L. E. P., Price-Whelan, A., and Newman, D. K. (2010). Phenazines affect biofilm formation by *Pseudomonas aeruginosa* in similar ways at various scales. *Res. Microbiol.* 161, 187–191. doi: 10.1016/j.resmic.2010.01.003
- Schneider, C. A., Rasband, W. S., and Eliceiri, K. W. (2012). NIH Image to ImageJ: 25 years of image analysis. *Nat. Methods* 9, 671–675. doi: 10.1038/nmeth.2089
- Sepúlveda-Torres, L., Huang, A., Kim, H., and Criddle, C. S. (2002). Analysis of regulatory elements and genes required for carbon tetrachloride degradation in *Pseudomonas stutzeri* strain KC. *J. Mol. Microbiol. Biotechnol.* 4, 151–161.
- Serventi, F., Ramazzina, I., Lamberto, I., Puggioni, V., Gatti, R., and Percudani, R. (2010). Chemical basis of nitrogen recovery through the ureide pathway: formation and hydrolysis of S-ureidoglycine in plants and bacteria. *ACS Chem. Biol.* 5, 203–214. doi: 10.1021/cb900248n
- Shen, X., Hu, H., Peng, H., Wang, W., and Zhang, X. (2013). Comparative genomic analysis of four representative plant growth-promoting rhizobacteria in *Pseudomonas*. *BMC Genomics* 14:271. doi: 10.1186/1471-2164-14-271
- Silby, M. W., Winstanley, C., Godfrey, S. A. C., Levy, S. B., and Jackson, R. W. (2011). *Pseudomonas* genomes: diverse and adaptable. *FEMS Microbiol. Rev.* 35, 652–680. doi: 10.1111/j.1574-6976.2011.00269.x
- Sitnikov, D. G., Monnin, C. S., and Vuckovic, D. (2016). Systematic assessment of seven solvent and solid-phase extraction methods for metabolomics analysis of human plasma by LC-MS. *Sci. Rep.* 6:38885. doi: 10.1038/srep38885
- Sørensen, J., and Nybroe, O. (2004). “*Pseudomonas* in the Soil Environment,” in *Pseudomonas: Volume 1 Genomics, Life Style and Molecular Architecture*, ed. J.-L. Ramos (Boston, MA: Springer), 369–401. doi: 10.1007/978-1-4419-9086-0_12
- Swenson, T. L., Karaoz, U., Swenson, J. M., Bowen, B. P., and Northen, T. R. (2018). Linking soil biology and chemistry in biological soil crust using isolate exometabolomics. *Nat. Commun.* 9:19. doi: 10.1038/s41467-017-02356-9
- Vaccaro, B. J., Lancaster, W. A., Thorgersen, M. P., Zane, G. M., Younkin, A. D., Kazakov, A. E., et al. (2016). Novel Metal Cation Resistance Systems from Mutant Fitness Analysis of Denitrifying *Pseudomonas stutzeri*. *Appl. Environ. Microbiol.* 82, 6046–6056. doi: 10.1128/AEM.01845-16
- Van Der Drift, L., Vogels, G. D., and Van Der Drift, C. (1975). Allantoin racemase: a new enzyme from *Pseudomonas* species. *Biochim. Biophys. Acta Enzymol.* 391, 240–248. doi: 10.1016/0005-2744(75)90170-9
- Viggiani, A., Olivieri, G., Siani, L., Di Donato, A., Marzocchella, A., Salatino, P., et al. (2006). An airlift biofilm reactor for the biodegradation of phenol by *Pseudomonas stutzeri* OX1. *J. Biotechnol.* 123, 464–477. doi: 10.1016/j.jbiotec.2005.12.024
- Wang, D., Xu, A., Elmerich, C., and Ma, L. Z. (2017). Biofilm formation enables free-living nitrogen-fixing rhizobacteria to fix nitrogen under aerobic conditions. *ISME J.* 11, 1602–1613. doi: 10.1038/ismej.2017.30
- Want, E. J., O’Maille, G., Smith, C. A., Brandon, T. R., Uritboonthai, W., Qin, C., et al. (2006). Solvent-dependent metabolite distribution, clustering, and protein extraction for serum profiling with mass spectrometry. *Anal. Chem.* 78, 743–752. doi: 10.1021/ac051312t
- Wetmore, K. M., Price, M. N., Waters, R. J., Lamson, J. S., He, J., Hoover, C. A., et al. (2015). Rapid quantification of mutant fitness in diverse bacteria by sequencing randomly bar-coded transposons. *mBio* 6:e00306-15. doi: 10.1128/mBio.00306-15
- Yan, Y., Ping, S., Peng, J., Han, Y., Li, L., Yang, J., et al. (2010). Global transcriptional analysis of nitrogen fixation and ammonium repression in root-associated *Pseudomonas stutzeri* A1501. *BMC Genomics* 11:11. doi: 10.1186/1471-2164-11-11

- Yao, Y., Sun, T., Wang, T., Ruebel, O., Northen, T., and Bowen, B. P. (2015). Analysis of metabolomics datasets with high-performance computing and metabolite atlases. *Metabolites* 5, 431–442. doi: 10.3390/metabo5030431
- Zhao, Y., Qu, D., Zhou, R., Yang, S., and Ren, H. (2016). Efficacy of forming biofilms by *Pseudomonas migulae* AN-1 toward in situ bioremediation of aniline-contaminated aquifer by groundwater circulation wells. *Environ. Sci. Pollut. Res. Int.* 23, 11568–11573. doi: 10.1007/s11356-016-6737-7

Conflict of Interest: MR and MZ, currently employed at DiCe Molecules and Molecular Devices, respectively, were not employed there at the time of the study.

The remaining authors declare that the research was conducted in the absence of any commercial or financial relationships that could be construed as a potential conflict of interest.

Publisher's Note: All claims expressed in this article are solely those of the authors and do not necessarily represent those of their affiliated organizations, or those of the publisher, the editors and the reviewers. Any product that may be evaluated in this article, or claim that may be made by its manufacturer, is not guaranteed or endorsed by the publisher.

Copyright © 2021 Kosina, Rademacher, Wetmore, de Raad, Zemla, Zane, Zulovich, Chakraborty, Bowen, Wall, Auer, Arkin, Deutschbauer and Northen. This is an open-access article distributed under the terms of the Creative Commons Attribution License (CC BY). The use, distribution or reproduction in other forums is permitted, provided the original author(s) and the copyright owner(s) are credited and that the original publication in this journal is cited, in accordance with accepted academic practice. No use, distribution or reproduction is permitted which does not comply with these terms.